J. CHEM. SOC. FARADAY TRANS., 1994, 90(16), 2337–2344

Hydroxylamine–Water: Intermolecular Potential Function and Simulation of Hydrated NH_2OH

Sergi Vizoso, Michael G. Heinzle and Bernd M. Rode
Institute for General, Inorganic and Theoretical Chemistry, University of Innsbruck, Innrain 52a, A-6020 Innsbruck, Austria

Two analytical pair-potential functions for NH_2OH–H_2O have been derived using 6-31G and 6-31G** basis sets for *ab initio* calculations of the interaction energy surface. The results of the *ab initio* calculations, and Monte Carlo simulations performed with these potentials, prove the importance of the polarization functions in potential construction. The hydration structure of NH_2OH is discussed on the basis of the Monte Carlo simulations.

1. Introduction

Monte Carlo and molecular dynamics techniques have been used extensively in studies of liquid systems at the molecular level.[1–9] Such studies gain particular importance when experimental data are not easily available. The reliability of these studies depends strongly on the quality of the potential functions which are usually obtained from SCF energy surfaces. Hence the results of the simulations also depend on the quality of the SCF calculations.

The first step in the studies presented here was to develop an analytical function describing the intermolecular interactions for NH_2OH–H_2O. This function was constructed from *ab initio* MO-SCF calculations of numerous points of the interaction energy surface. We have compared two series of *ab initio* SCF calculations and their corresponding potential functions using an identical basis set with and without polarization functions.

Provided a suitable potential function is obtained, it will allow a series of simulations of mixed hydroxylamine–water systems, whose properties as a mixed solvent for electrolytes are as interesting as the microstructures formed in such liquids. Experimental structural data for the system treated here are not available and could be obtained only by rather laborious X-ray and neutron diffraction studies, which have not been reported so far.

2. Computational Details

2.1 Geometries and Basis Set

For the evaluation of the complete energy surface describing the interaction of water and hydroxylamine molecules, a large number of *ab initio* calculations is needed. Therefore, it seemed appropriate to perform some test calculations on various adducts of the two species in order to determine whether a medium-sized basis set could ensure sufficient accuracy for this purpose while keeping computational efforts at a reasonable level. The internal molecular geometry parameters for hydroxylamine and water (Table 1) were taken from previous calculations,[10–13] where larger basis sets were used. Since a potential for rigid molecules was to be constructed, the internal geometry of both molecules was also kept fixed during these test calculations, and only intermolecular distances and angles were optimized. The use of 'flexible' intramolecular geometries did not appear necessary since the comparison of molecular dynamics simulations[12] of the aqueous system using non-rigid and Monte Carlo simulations[14] of the same systems with rigid geometries did not produce significant differences.

The first series of calculations was carried out using the split-valence-shell basis set 6–31G developed by Gordon[15] and Pople and co-workers,[16,17] consisting of 86 primitive functions, 10s 4p/[3s 2p] for oxygen and nitrogen, and 4s/[2s] for the hydrogen atoms. In order to study the influence of polarization functions in the basis set on pair potential derivation, the same energy points were re-evaluated using the 6–31G** basis set (11s 4p 1d/[4s 2p 1d] for nitrogen and oxygen atoms, and 4s 1p/[2s 1p] for hydrogen) where the standard exponents ($\alpha_p = 1.1$, $\alpha_d = 0.8$) and no scaling factor ($\xi = 1.0$) were used in the uncontracted polarization functions. This basis set has been used frequently as a compromise between accuracy and computational effort and has generally led to reliable molecular geometries.

A comparison of the results derived from these basis sets for some relevant adducts with more extended SCF calculations using the triple zeta + polarization basis set 6–311G** (Table 2) shows that stabilization energies are considerably overrated with the 6–31G basis set (due to too short intermolecular distances), but quite similar when polarization functions are added. The relative order of stability for the relevant adducts is also preserved in this case, which is of crucial importance for the generation of an appropriate pair-potential function. A possible source of error, especially for the smallest basis set, would be the basis set superposition error (BSSE), which has been estimated by Boys and Bernardi.[18] The results for both 6–31G and 6–31G** basis sets are quite similar, however, and it is observed that the BSSE plays a significant role only at short distances where the potential is already repulsive. An estimation of the upper BSSE limit at the global minimum leads to values of 1.6 kcal mol^{-1} without, and 1.8 kcal mol^{-1} with, polarization functions. For other local minima on energy surfaces, corrected and uncorrected energies differ even less. It is obvious, therefore, that differences in BSSE do not account for the improvement of stabilization energies by the inclusion of polarization functions. For this reason, and bearing in mind extensive discussions in the literature pointing out that the counterpoise corrected energy is not necessarily more reliable than the uncorrected one,[19–47] a BSSE correction of potential surface points did not appear necessary or advantageous.

Table 1 Geometry and partial charges for hydroxylamine[10,11] and water[12,13,51]

bond length/Å		bond angle/degrees		charge/*e*	
		NH_2OH			
N—O	1.453	HNH	107.1	N	−0.482
N—H_N	1.017	HNO	103.2	H_N	0.301
O—H_O	0.962	HON	101.4	O	−0.525
				H_O	0.405
		H_2O			
O—H	0.96	HOH	104.5	O	−0.660
				H	0.330

Table 2 Most stable adduct geometries: (*a*) *ab initio* calculations using 6-31G basis set

geometry	bond length/Å N—O	bond angle/degrees NO—O	bond angle/degrees N—HO	dihedral angle NOH—O	stabilization energy/kcal mol^{-1}	figure ref.
HN···H	2.837	76.9	124.5	1.2	−9.3	2(*a*)
HO···H	3.025	84.9	106.9	−93.5	−7.9	2(*b*)
NH···O(1)	2.974	82.8	102.9	−91.7	−7.9	2(*c*)
NH···O(2)	2.997	83.4	104.7	92.7	−7.9	2(*d*)
OH···O	3.088	89.3	85.4	0.0	−8.3	2(*e*)

(*b*) *Ab initio* calculations using 6-31G** basis set

geometry	bond length/Å N—O	bond angle/degrees NO—O	bond angle/degrees N—HO	dihedral angle NOH—O	stabilization energy/kcal mol^{-1}	figure ref.
HN···H	2.924	76.2	131.1	0.0	−7.5	2(*a*)
HO···H	3.137	85.5	111.8	−92.4	−6.3	2(*b*)
NH···O(1)	3.115	84.1	109.0	−91.3	−6.2	2(*c*)
NH···O(2)	3.117	84.2	109.1	91.5	−6.2	2(*d*)
OH···O	3.207	89.5	86.4	−1.5	−5.4	2(*e*)

(*c*) *Ab initio* calculations using 6-311G** basis set

geometry	bond length/Å N—O	bond angle/degrees NO—O	bond angle/degrees N—HO	dihedral angle NOH—O	stabilization energy/kcal mol^{-1}	figure ref.
HN···H	2.925	76.1	130.8	0.0	−7.3	2(*a*)
HO···H	3.144	85.8	111.2	−93.0	−6.2	2(*b*)
NH···O(1)	3.120	84.5	108.7	−92.2	−6.1	2(*c*)
NH···O(2)	3.121	84.5	108.8	92.2	−6.1	2(*d*)
OH···O	3.205	89.3	87.0	−1.3	−5.6	2(*e*)

A second source of error could be the neglect of correlation energy. This issue has been investigated already in the construction of the NH_2OH–NH_2OH potential,[10] leading to the conclusion that balanced basis sets of DZP, or similar quality, reflect correctly the relative stabilization of various hydrogen-bonded adducts and also produce (sometimes due to fortunate error compensation) acceptable absolute values. We therefore evaluated the correlation contribution for the global and nearest local minimum on the energy surface at MP2/6–311G** level, obtaining a decrease of stabilization energy of 0.4 and 0.3 kcal mol^{-1}, respectively. These values do not justify the enormously higher computational effort for evaluating all the surface points at this level.

The possible influence of three-body effects still remains open for discussion; considering binding distances and interaction energies as well as the very small influence of the three-body effects in the case of pure water,[48] it can be assumed that they have no significant impact on the simulation results, at least on structural data, which will represent the main target of subsequent investigations.

It was decided, therefore, to evaluate the pair potential for both split-valence basis sets, without (A) and with (B) polarization functions, the objective being to study whether the errors encountered for energy values and intermolecular distances while omitting the polarization functions, would have a serious influence on structural data of the simulated liquid, or whether the generally not so sensitive radial distribution functions (RDF) would still give an acceptable representation of the microstructures formed in the condensed system. In that case, a further considerable reduction in computational effort could be achieved, which would be of importance especially for larger systems than the one considered here.

2.2 Selection of Adduct Geometries

In order to have a complete representation of the potential surface, the following surface points were generated: keeping the hydroxylamine molecule fixed, the water molecule was positioned at locations within 15 Å, varying the angular orientations for each of these points. Special attention was paid to the chemically significant configurations allowing the formation of hydrogen bonds, and configuration optimization was carried out for all hydrogen-bonded local minima. By this procedure, over 1000 energy points were computed for both energy surfaces.

All *ab initio* calculations were carried out using GAUSSIAN 92.[49]

2.3 *Ab initio* Results

A comparison with previous calculations[50] showed that the global minimum found for potential surface B is in good agreement with the most stable configuration found for NH_2OH–H_2O by Yeo and Ford, who have used the same basis set at second-order Møller–Plesset perturbation theory level (MP/2).

In order to compare the results for both basis sets A and B, several potential curves for representative configurations [Fig. 1(*d*) and (*e*) represent direct hydrogen-bond interactions and Fig. 1(*f*) is an aligned molecular dipole moment configuration] were plotted. From Fig. 1(*a*)–(*c*) the difference in the locations of energy minima (0.2 Å in configurations 1 and 2, and 0.1 Å in configuration 3) and in the associated stabilization energies may be observed, especially for configurations 1 and 2 with direct hydrogen bonding (2–2.5 kcal mol^{-1} too low). Also at larger distances 6–31G curves show over-stabilization compared with 6–31G** data. Besides these effects, calculations without polarization functions also alter the slope of the potential curves and the geometry of the adducts [Tables 2(*a*) and 2(*b*)]. Their configurations are presented in Fig. 2, hydrogen bonding being marked by dotted lines.

The shorter equilibrium distances result from an enhanced Coulomb interaction due to overestimation of permanent

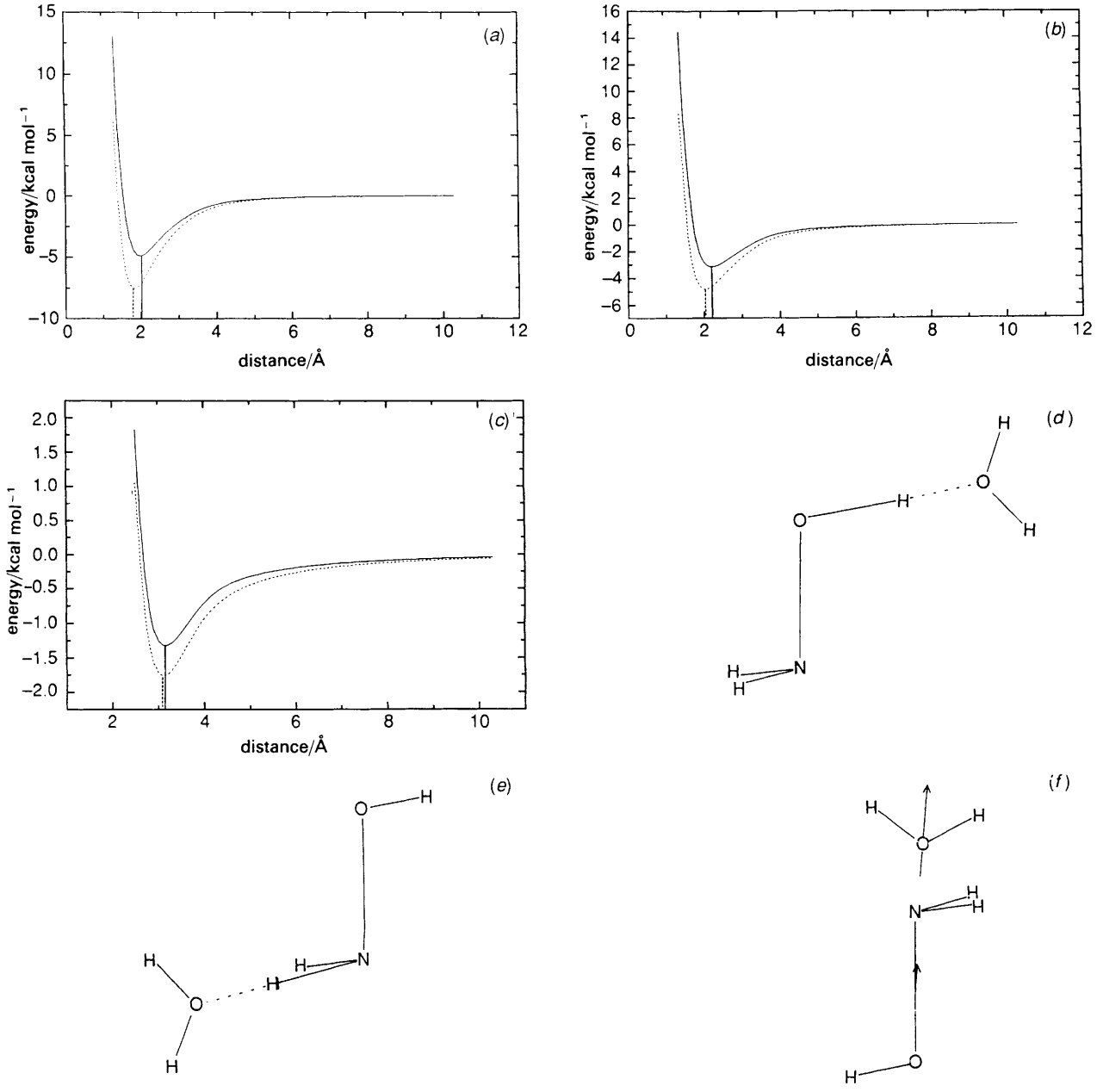

Fig. 1 SCF potential curves calculated with and without polarization functions: (*a*) $H_O\cdots O$ by 6–31G** (——) and 6–31G (– – –); (*b*) $H_N\cdots O$ by 6–31G* (——) and 6–31G (– – –); (*c*) dipole oriented ($\mu\cdots\mu$), 6–31G** (——) and 6–31G (– – –); (*d*) view of $H_O\cdots O$ configuration; (*e*) view of $H_N\cdots O$ configuration; (*f*) view of dipole oriented ($\mu\cdots\mu$) configuration

dipole moments of the molecules (+41% for water and +56% for hydroxylamine, *cf.* Table 3). Another effect is the underestimation of the electronic repulsion between both species due to the omission of polarization functions, allowing too close an approach of the interacting partners.

Table 3 Dipole moments for water and hydroxylamine

	H_2O		NH_2OH	
dipole moment/D[a]	μ_{total}	%dif[b]	μ_{total}	%dif[b]
6–31G	2.632	40.8	0.918	55.6
6–31G*	2.228	19.2	0.779	32.1
6–31G**	2.188	17.0	0.777	31.8
6–311G**	2.169	16.0	0.799	35.4
experimental	1.87	—	0.59	—

[a] 1 D (Debye) $\approx 3.335\,64 \times 10^{-30}$ C m. [b] Percentage difference between calculated and experimental values.

3. Fitting of Intermolecular Pair-potential Functions

3.1 Fitting Procedure

The SCF energy points were fitted to an analytical function which depends on atomic coordinates and contains a Coulomb, an exponential and several r^{-n} terms. Such a function implies pairwise additivity and therefore the total interaction energy is expressed as a sum of the atom–atom pair potentials, each depending exclusively on the distance r_{ij} between both the atoms considered.

The original potential function form was:

$$\Delta U_{total} = \sum_i \sum_j \Delta U_{ij} = \sum_i \sum_j \left[Q_{ij} \frac{q_i q_j}{r_{ij}} + A_{ij} \exp(-B_{ij} r_{ij}) + \sum_a \frac{C_{ij}^a}{r_{ij}^n} \right]$$

in which the first term represents the Coulomb interaction

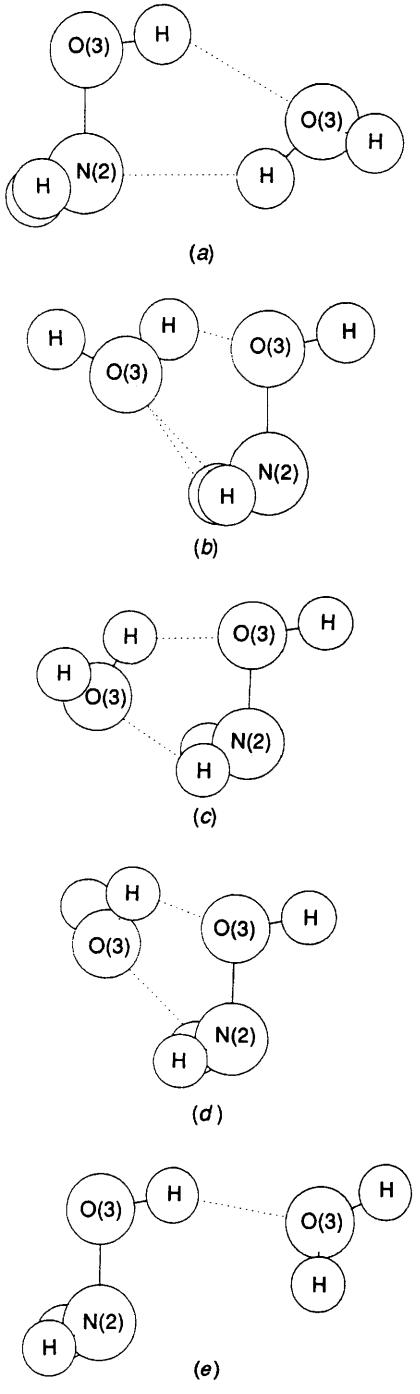

Fig. 2 View of the five most stable adducts. Hydrogen bonding is represented by the dotted lines.

between the partial charges of atoms i and j. The number and type of r^{-n} terms was varied in order to obtain optimal fitting conditions.

For the fractional atomic charges obtained by Mulliken population analysis it was observed, especially for the larger basis sets, that they have quite similar values to the monomer; the differences range from −0.05 to 0.08e†. Consequently, the atomic partial charges were assigned their monomer values (*cf.* Table 1), which were obtained from previous more extended *ab initio* calculations[11,51] and were kept fixed during the fitting process. The remaining charge fluctuations should be taken care of by the lower r^{-n} terms. Thus all

† $1\ e \approx 1.602\,18 \times 10^{-19}$ C.

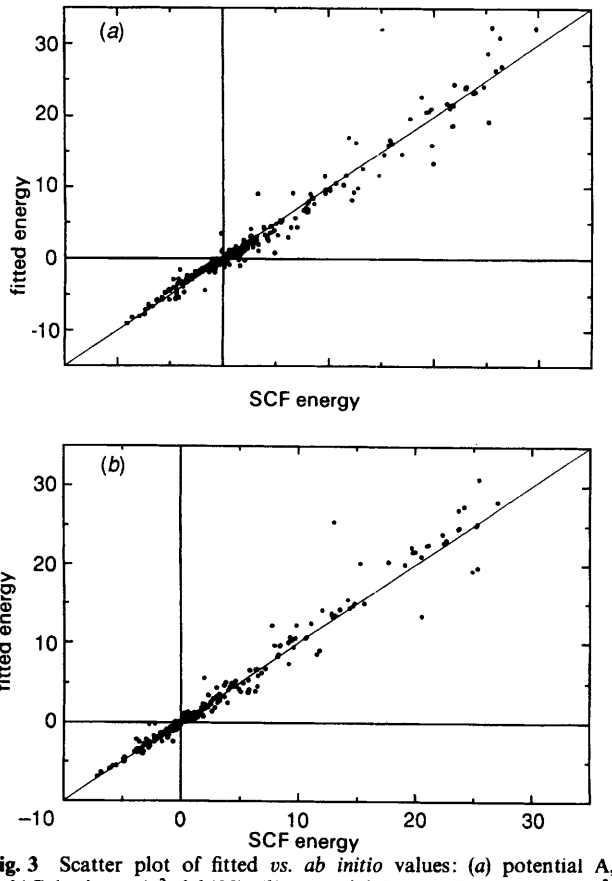

Fig. 3 Scatter plot of fitted *vs. ab initio* values: (*a*) potential A, 6–31G basis set (χ^2, 0.0428); (*b*) potential B, 6–31G** basis set (χ^2, 0.0424)

parameters Q_{ij} for the Coulombic term of the pair potential were set to one and not modified during the fitting procedure. This procedure is not only convenient but also gives charge consistency with the hydroxylamine–hydroxylamine and water–water potentials used in subsequent Monte Carlo simulations.

Although the use of these monomer charges for hydroxylamine results in a relatively large molecular dipole moment when compared with the experimental value,[11] it is known that overestimated values for dipole moments seem to be of advantage for simulations of liquid systems.[52] The reasons for this phenomenon are charge redistributions induced in the liquid due to interactions of more than two molecules, which enlarge the dipole moments of the molecules.

The fitting procedure was performed by minimizing the sum of the squared differences between the fitted and *ab initio* energy values first by a steepest-descent algorithm followed by a Newton–Raphson algorithm. Points above 30 kcal molecule^{-1} were excluded and weighting was performed with respect to the absolute and low-lying local minima. The quality of the fit was checked by its statistical properties (standard deviations, residuals, χ^2), the energy minima (checking for possible distance shifts), the relative hierarchy of local minima for chemically important configurations and by a graphical representation of fitted energies *vs.* SCF values. The predictive capability of both potential functions was then tested by calculating 40 additional configurations not included in the first set and comparing them with the corresponding values predicted by the function.

3.2 Fitting Results

It was found that for both series the best fitting results are obtained using three r terms with 3, 6 and 9 as exponents, in

Table 4 (*a*) Fitted parameters obtained with 6–31G basis set (potential A)

pair	A/kcal mol^{-1}	B/Å^{-1}	C/kcal Å^3 mol^{-1}	D/kcal Å^6 mol^{-1}	E/kcal Å^9 mol^{-1}
N···O	3811.920 66	2.422 22	217.180 88	0.021 21	1.983 87
N···H	4.793 69	0.208 06	−189.741 39	475.983 62	0.166 22
H_N···O	−5424.282 59	4.707 42	−131.099 58	287.748 42	195.219 74
H_N···H	74.066 01	1.315 73	8.159 77	34.877 37	0.053 22
O···O	140.720 65	0.638 99	−681.490 72	5172.394 74	5.980 44
O···H	26.808 81	0.783 12	−125.170 42	395.527 41	1.705 95
H_O···O	7076.106 81	3.977 02	−95.994 69	0.005 10	0.124 37
H_O···H	73.073 01	1.277 21	−14.265 08	49.239 49	0.170 55

(*b*) Fitted parameters obtained with 6–31G** basis set (potential B)

pair	A/kcal mol^{-1}	B/Å^{-1}	C/kcal Å^3 mol^{-1}	D/kcal Å^6 mol^{-1}	E/kcal Å^9 mol^{-1}
N···O	958.189 98	2.289 58	271.719 41	637.683 33	2281.781 06
N···H	3.435 69	0.179 03	−175.692 85	511.789 96	153.928 73
H_N···O	−90626.018 29	5.663 26	−147.148 65	588.307 58	107.661 76
H_N···H	78.998 89	1.600 58	12.366 92	17.493 45	2.814 23
O···O	139.636 12	0.673 38	−669.91 12	4671.420 94	27.652 35
O···H	34.655 35	0.767 86	−88.595 18	318.249 04	4.685 96
H_O···O	3132.775 92	3.233 41	−90.508 07	0.087 17	8.147 61
H_O···H	110.203 53	2.207 77	11.486 71	0.355 99	2.157 74

addition to the Coulomb and the exponential term. Therefore the final pair-potential function is:

$$\Delta U_{\text{total}} = \sum_i \sum_j \left[\frac{q_i q_j}{r_{ij}} + A_{ij} \exp(-B_{ij} r_{ij}) + \frac{C_{ij}}{r_{ij}^3} + \frac{D_{ij}}{r_{ij}^6} + \frac{E_{ij}}{r_{ij}^9} \right]$$

This potential form provided very satisfactory overall fitting results. The standard deviation obtained was below 0.043 in both cases and, more important, the distance, shape and order of local minima was maintained, which is crucial for correct simulation results. The final optimized parameters are presented in Tables 4(*a*) and (*b*). Accuracy is particularly good near the potential surface minima, owing to the inclusion of weighting parameters. Fig. 3(*a*) and (*b*) show the scatterplot of fitted *vs.* SCF calculated energy data. The test of fitting quality by the inclusion of additional randomly chosen SCF points, described previously, and comparison with the corresponding predicted values also proved the reliability and completeness of the potential function.

4. Monte Carlo Simulations

4.1 Method and System

A simulation for five hydroxylamine and 195 water molecules was carried out with both potentials using a modified version of the MC92 programme.[53] Water–water interactions were calculated by the CF2 potential[51] while the potential developed by Michopoulos *et al.*[10] was taken to evaluate hydroxylamine–hydroxylamine pair energies.

The basic box containing the five hydroxylamine and 195 water molecules corresponds to a 1.3687 mol dm^{-3} or 4.46% solution of hydroxylamine. The elementary box length was evaluated to be 18.238 Å from the corresponding mixed liquid system density at 20 °C (1.0068 g cm^{-3}, obtained by interpolation of bibliographical data[54]). The simulation was carried out with the Metropolis algorithm[55] and periodic boundary conditions under minimal image convention,[56] and for the exponential term, a spherical cut-off of half the box length was applied. The long-range Coulomb forces were approximated by means of Ewald summation, using a value of $\varepsilon = \infty$ for the surrounding medium. Initial positions for the molecules were generated randomly, and the system needed about 2×10^6 steps before equilibrium was reached. The ratio of accepted : rejected configurations was adjusted to the value of 0.5 by continuous adaptation of maximum shift and turn parameters. A further 1×10^6 configurations were used for sampling.

All *ab initio* calculations and Monte Carlo simulations were done on IBM 550 and DEC 3100 workstations at our institute.

4.2 Monte Carlo Simulation Results

The structure of the solution was evaluated based on radial distribution functions (RDF) and running integration numbers. The characteristic data (maxima, minima and coordination numbers) are given in Tables 5(*a*) and (*b*). RDF plots are presented in Fig. 4 and 5.

Both simulations lead to similar average coordination numbers and structural results, but the radial density functions have quite different shapes. This is clearly a consequence of the overestimation of permanent dipole moments and underestimation of polarization effects without d-functions in the basis set.

In general terms the system structure around NH_2OH appears as a large hydration shell ($R_{ij} \in$ 4.5–5.0 Å) involving an average of 16 or 17 water molecules distributed in two semi-shells each containing eight water molecules, and being oriented around O and N of the hydroxylamine molecule. This high coordination number can be attributed to the rather large size of the hydroxylamine molecule and the low stabilization energy of hydrogen-bonded structures, which makes binding flexible enough to allow other molecules to be placed within this first shell.

4.2.1 *RDFs*

The shorter equilibrium distances obtained for potential A (*ca.* 0.3–0.5 Å, reflected by RDF peak positions) are clearly a consequence of the underestimation of electronic repulsion and of high permanent dipole moments which allow too close an approach of the interacting molecules, resulting in an enlarged Coulomb term and thus in too low energy values. Potential A overemphasizes hydrogen-bonded structures at short distances, visible from additional peaks at

Table 5 (*a*) Radial distribution function characteristics obtained with potential A

RDF	peak 1[a]	n_{p1}	M_1	m_1	n_1
N—O	2.9	2	3.5	5.2	17.5
N—H	2.0	0.4	3.5	4.85	16
O—O	—	—	2.8	4.3	10
O—H	2.05	1	2.7	3.9	7
H_N—O	2.1	1	3.5	5.0	16
H_O—O	1.9	1.4	3.1	4.0	8

(*b*) Radial distribution function characteristics obtained with potential B

RDF	peak 1[a]	n_{p1}	M_1	m_1	n_1	m_2	n_2
N—O	—	—	3.35	3.85	8	5.05	17.5
N—H	2.3	0.5	3.9	5.7	47[c]	—	—
O—O	—	—	3.0	3.9	8	5.0	16
O—H	2.1	1	3.0	5.0	32[c]	—	—
H_N—O	2.4	1.8	3.75	5.0	17.5	—	—
H_O—O	2.1	1	3.2	4.6	11.5	—	—

[a] These data correspond either to a split-off peak or a shoulder. [b] First integration number n_{p1} corresponds to integration values for peak 1 and represents direct hydrogen-bonding interactions. Second and third integration numbers, n_1 and n_2, reflect integration values up to first (m_1) and second minimum (m_2). The position of the main maximum is given as M_1. [c] In the integration process both water hydrogens are taken into account.

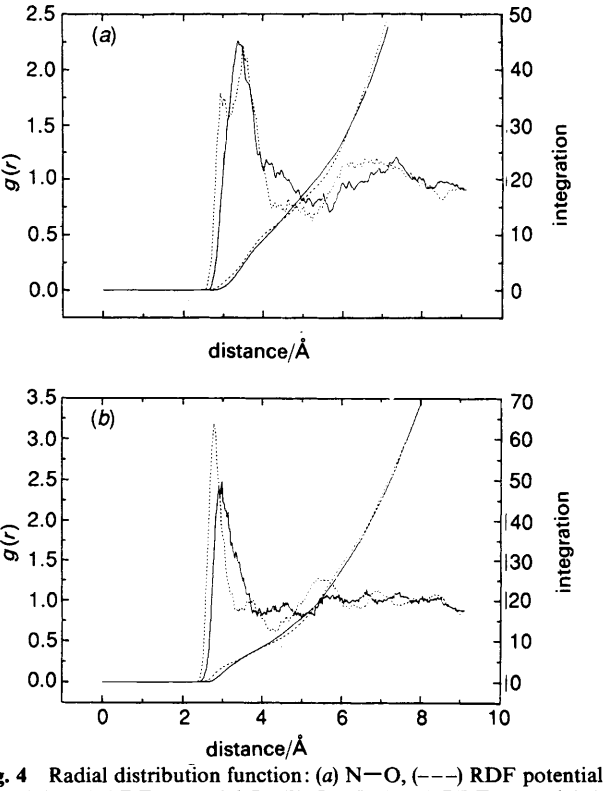

Fig. 4 Radial distribution function: (*a*) N—O, (– – –) RDF potential A and (——) RDF potential B; (*b*) O—O, (– – –) RDF potential A and (——) RDF potential B

about 2 Å in the RDFs presented in Fig. 5. From these results it can be concluded that potential A does not describe the system accurately, and ultimately leads to false structural information. Therefore, only potential B will be used for further discussion of the liquid microstructure.

From N—O and O—O RDF pictures (Fig. 4) the arrangement of water around hydroxylamine can be determined. The first peaks of these RDFs located around 3 Å reflect the existence of eight water molecules close to N and O, respectively, Table 5(*b*), and a further, not clearly separate zone, which includes N-bonded water molecules in O—O RDF and O-

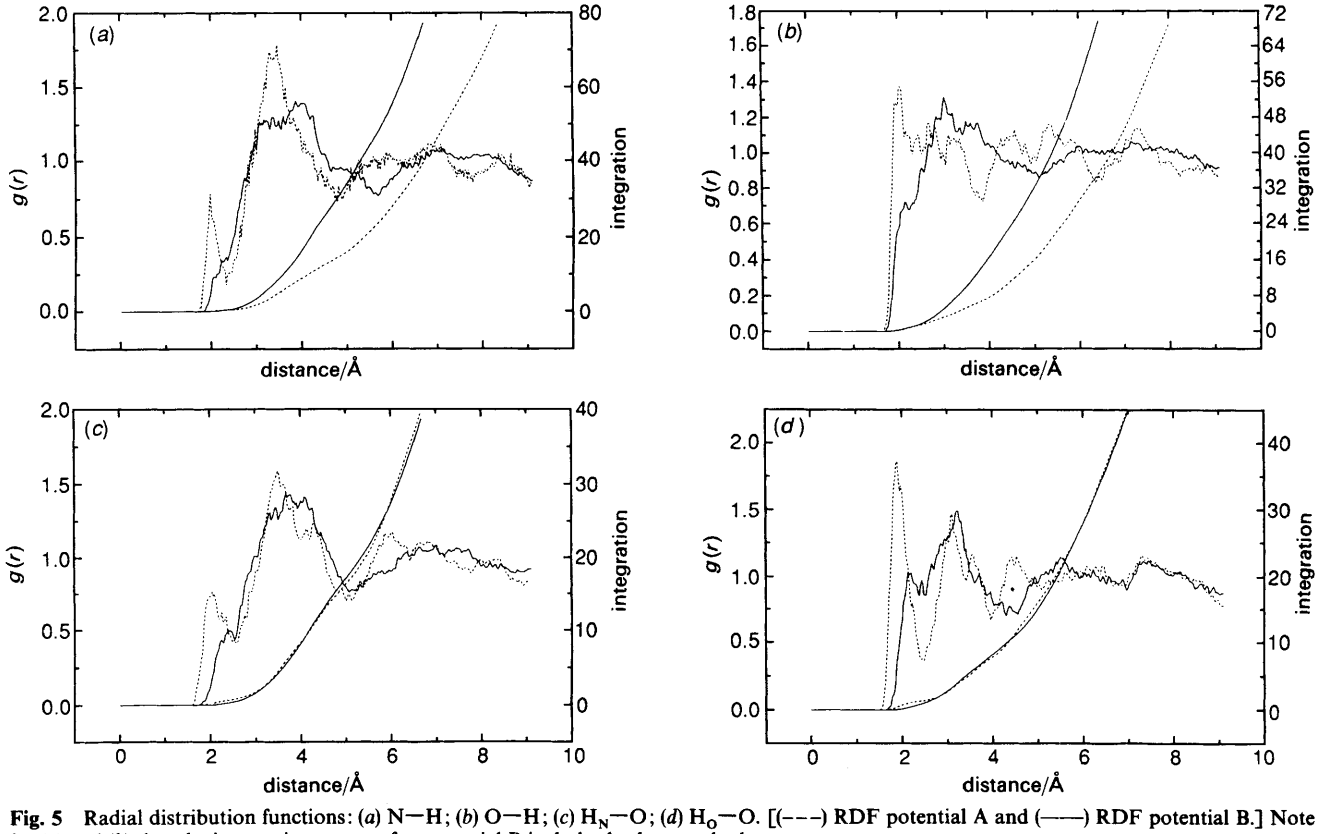

Fig. 5 Radial distribution functions: (*a*) N—H; (*b*) O—H; (*c*) H_N—O; (*d*) H_O—O. [(– – –) RDF potential A and (——) RDF potential B.] Note for (*a*) and (*b*) that the integration process for potential B includes both water hydrogen atoms.

bonded water in the N—O RDF and extends from 4.0 to 5.0 Å, containing the other eight water molecules. The hydration structure around hydroxylamine appears, therefore, as a large shell containing 16 water molecules consisting of two *semi-shells* of eight molecules which are placed around oxygen and nitrogen. The hydrogen-bonding interactions, which have appeared as a split-off single peak at *ca.* 1.9–2.1 Å with potential A, are present as shoulders placed at larger distances (2.1–2.4 Å) in potential B RDFs (Fig. 5). Out of the 16 water molecules of the hydration shell an average number of 4–4.5 are hydrogen bonded [Table 5(*b*)] while the rest are mainly electrostatically interacting.

4.4.2 *Coordination Number and Energy Distributions*

In both simulations a value of *ca.* 16 was obtained as the main coordination number. Despite this coincidence the statistical coordination number distributions (Fig. 6) show some remarkable differences. Potential A's coordination number distribution is almost symmetric with respect to the average coordination number while for potential B's coordination number distribution, a more irregular histogram shifted to higher coordination values is obtained. This can be seen as a consequence of the shorter equilibrium distance obtained with potential A. The larger distances obtained with potential B are reflected in a major occupation of higher coordination numbers (27% for 17, 23% for 18 and 8% for 19) while the values obtained with potential A are considerably lower (23% for 17, 13% for 18 and 3% for 19). The pair-energy distribution functions (EDF) for the pairs within the large hydration shell ($r_{ij} \leqslant 5$ Å) are presented in Fig. 7. Although potential A gives more distinct RDF peaks for H-bonded configurations, the smaller diameter of the shell apparently does not allow the formation of distinct ideal hydrogen bonds. Therefore, the energy distribution is decreasing almost exponentially. Within the larger radius of potential B, such ideal H-bonded

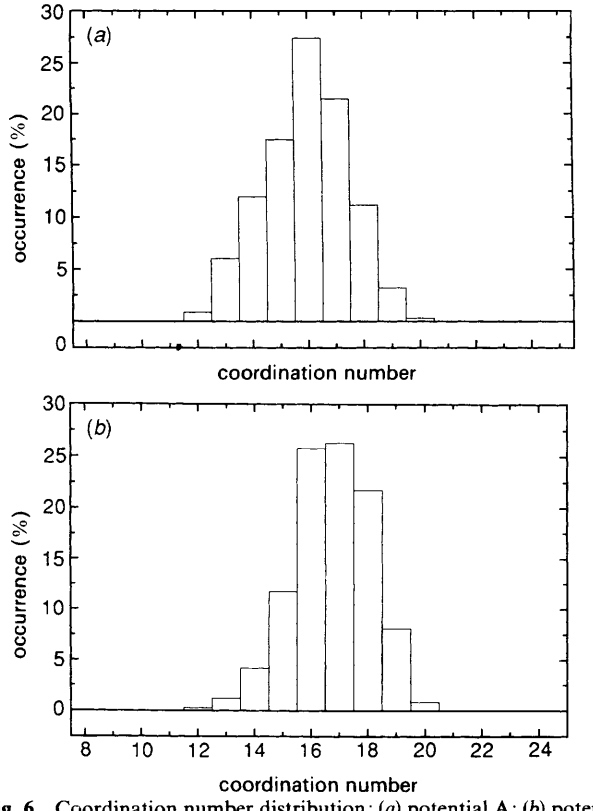

Fig. 6 Coordination number distribution: (*a*) potential A; (*b*) potential B. Limit distance, 5 Å.

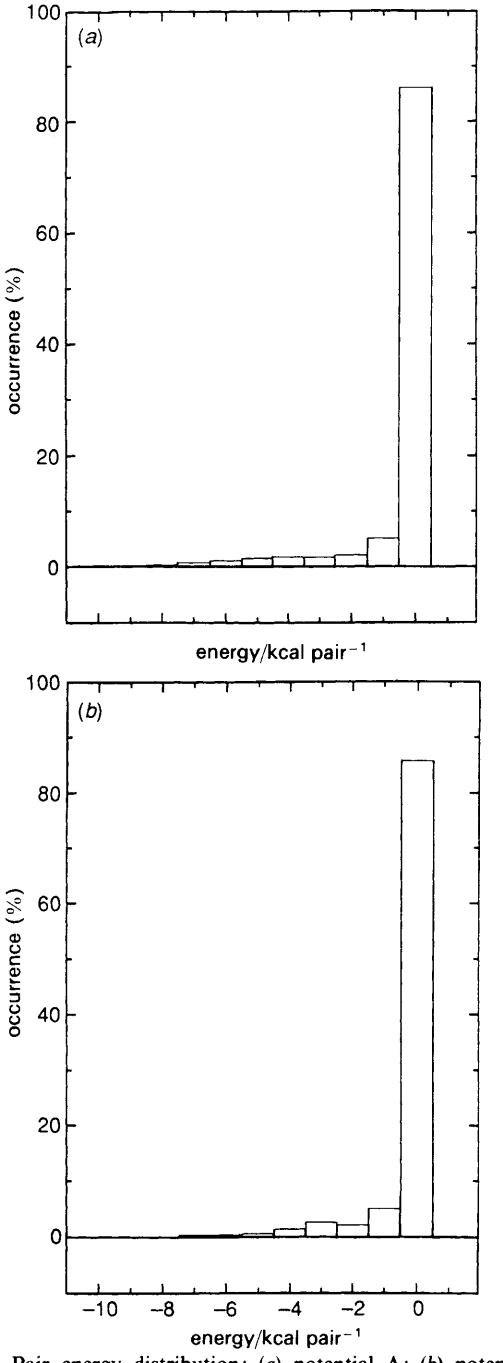

Fig. 7 Pair energy distribution: (*a*) potential A; (*b*) potential B. Limit distance, 5 Å.

configurations can be realized and are visible as a separate small maximum in the energy distribution histogram at a value of *ca.* 4 kcal pair^{-1}. Such configurations contribute, however, only to a very minor extent (*ca.* 5%) to the formation of the first hydration layer.

Conclusions

Polarization functions seem to be essential in order to obtain reliable potential functions of hydrogen-bonded systems. Moreover, their omission in the construction of the potential can also lead to significant deviations in Monte Carlo simulation results, even for RDFs which are usually considered to be less sensitive to the quality of the pair potential functions. It can be concluded, therefore, that double-zeta + polarization quality is a minimal requirement for the

evaluation of *ab initio*-based pair potentials also of larger hydrogen-bonded molecular systems.

Financial support by the Austrian Science Foundation (Project No. 9078 MOB) is gratefully acknowledged. Thanks are also due to the Austrian Federal Ministry for Science and Research and the Spanish Ministry for Education and Science for funding the bilateral cooperation.

References

1 R. W. Impey, M. Sprik and M. L. Klein, *J. Am. Chem. Soc.*, 1987, **109**, 5900.
2 B. M. Rode and S. M. Islam, *J. Chem. Soc., Faraday Trans. 1*, 1992, **88**, 417.
3 M. L. Klein, I. R. McDonald and R. Righini, *J. Chem. Phys.*, 1979, **71**, 3673.
4 D. J. Adams, *Chem. Phys. Lett.*, 1979, **62**, 329.
5 Y. P. Yongyai, S. Kokpol and B. M. Rode, *Chem. Phys.*, 1991, **159**, 403.
6 R. W. Impey and M. L. Klein, *Chem. Phys. Lett.*, 1984, **104**, 579.
7 K. P. Sagarik, R. Ahlrichs and S. Brode, *Mol. Phys.*, 1986, **57**, 1247.
8 J. Gao, *J. Phys. Chem.*, 1992, **96**, 537.
9 Y. Michopoulos and B. M. Rode, *Int. J. Quantum Chem.*, 1992, **42**, 1339.
10 Y. Michopoulos, P. Botschwina and B. M. Rode, *Z. Naturforsch., Teil A*, 1991, **46**, 32.
11 S. Tsunekawa, *J. Phys. Soc. Jpn.*, 1972, **33**, 167.
12 P. Bopp, W. Dietz and K. Heinzinger, *Z. Naturforsch., Teil A*, 1979, **34**, 1424.
13 W. Dietz, W. O. Riede and K. Heinzinger, *Z. Naturforsch., Teil A*, 1982, **37**, 1038.
14 J. P. Limtrakul, M. M. Probst and B. M. Rode, *J. Mol. Struct. Theochem*, 1985, **121**, 23.
15 M. S. Gordon, *Chem. Phys. Lett.*, 1980, **76**, 163.
16 W. J. Hehre, R. Ditchfield and J. A. Pople, *J. Chem. Phys.*, 1972, **56**, 2257.
17 P. C. Hariharan and J. A. Pople, *Theor. Chim. Acta*, 1973, **28**, 213.
18 S. Boys and F. Bernardi, *Mol. Phys.*, 1970, **19**, 553.
19 D. W. Schwenke and D. G. Truhlar, *J. Chem. Phys.*, 1985, **82**, 2418.
20 G. H. F. Diercksen, W. P. Kraemer and B. O. Roos, *Theor. Chim. Acta*, 1975, **36**, 249.
21 N. R. Kestner, M. D. Newton and T. L. Mathers, *Int. J. Quantum Chem. Symp.*, 1983, **17**, 431.
22 M. D. Newton and N. R. Kestner, *Chem. Phys. Lett.*, 1983, **94**, 198.
23 M. J. Frisch, J. E. Del Bene, J. S. Binkley and H. F. Schaefer III, *J. Chem. Phys.*, 1986, **84**, 2279.
24 H. J. Bohm and R. Ahlrichs, *Mol. Phys.*, 1985, **55**, 1159.
25 D. Kocjan, J. Koller and A. Azman, *J. Mol. Struct.*, 1976, **34**, 145.
26 B. Jonsson and B. Nelander, *Chem. Phys.*, 1977, **25**, 263.
27 G. M. Maggiora and I. H. Williams, *J. Mol. Struct.*, 1982, **88**, 23.
28 F. J. Olivares Del Valle, S. Tolosa, A. Lopez Pineiro and A. Requena, *J. Comput. Chem.*, 1985, **6**, 39.
29 J. P. Daudey, P. Claverie and J. P. Malrieu, *Int. J. Quantum Chem.*, 1974, **8**, 1.
30 E. Kochanski, in *Intermolecular Forces*, ed. B. Pullman, Reidel, Dordrecht, 1981, p. 15.
31 J. J. Bentley, *Am. Chem. Soc.*, 1982, **104**, 2754.
32 U. Wahlgren and L. Pettersson, *Chem. Phys.*, 1982, **69**, 185.
33 B. H. Wells and S. Wilson, *Mol. Phys.*, 1983, **50**, 1295.
34 B. H. Wells and S. Wilson, *Chem. Phys. Lett.*, 1983, **101**, 429.
35 P. W. Fowler and P. A. Madden, *Mol. Phys.*, 1983, **49**, 913.
36 P. W. Fowler and A. D. Buckingham, *Mol. Phys.*, 1983, **50**, 1349.
37 F. Spiegelmann and J. P. Malrieu, *Mol. Phys.*, 1980, **40**, 1273.
38 B. H. Lengsfield III, A. D. McLean, M. Yoshimine and B. Liu, *J. Chem. Phys.*, 1983, **79**, 1891.
39 M. Allavena, B. Silvi and J. Cipriani, *J. Chem. Phys.*, 1982, **76**, 4573.
40 E. Miyoshi, H. Tatewaki and T. Nakamura, *J. Chem. Phys.*, 1983, **78**, 815.
41 J. Andzelm, M. Klobukowski and E. Radzio-Andzelm, *J. Comput. Chem.*, 1984, **5**, 146.
42 I. C. Hayes, G. J. B. Hurst and A. J. Stone, *Mol. Phys.*, 1984, **53**, 107.
43 U. E. Senff and P. G. Burton, *J. Phys. Chem.*, 1985, **89**, 797.
44 J. R. Collins and G. A. Gallup, *Chem. Phys. Lett.*, 1986, **123**, 56; 1986, **129**, 329.
45 M. D. Newton, *J. Chem. Phys.*, 1983, **87**, 4288.
46 J. H. van Lenthe, T. van Dam, F. B. van Duijneveldt and L. M. J. Kroon-Batenburg, *Faraday Symp. Chem. Soc.*, 1984, **19**, 125.
47 P. Hobza, B. Schneider, P. Carsky and R. Zahradnik, *J. Mol. Struct. Theochem*, 1986, **138**, 377.
48 G. C. Lie, E. Clementi and M. Yoshimine, *J. Chem. Phys.*, 1976, **64**, 2314.
49 M. J. Frisch, G. W. Trucks, M. Head-Gordon, P. M. W. Gill, M. W. Wong, J. B. Foresman, B. G. Johnson, H. B. Schlegel, M. A. Robb, E. S. Replogle, R. Gomperts, J. L. Andres, K. Raghavachari, J. S. Binkley, C. Gonzalez, R. L. Martin, D. J. Fox, D. J. Defrees, J. Barker, J. J. P. Stewart and J. A. Pople, GAUSSIAN 92, Revision B, Gaussian Inc., Pittsburgh PA, 1992.
50 G. A. Yeo and T. A. Ford, *J. Mol. Struct.*, 1991, **235**, 123.
51 G. Jancso, K. Heinzinger and P. Bopp, *Z. Naturforsch., Teil A*, 1985, **40**, 1235.
52 E. H. S. Anwander, M. M. Probst and B. M. Rode, *Chem. Phys.* 1992, **166**, 341.
53 M. G. Heinzle and B. M. Rode, Program MC92, produced by Project P8475-MOB, University of Innsbruck, 1992.
54 LANDOLT-BÖRNSTEIN, *Numerical Data and Functional Relationships in Science, New Series*, Group IV, Springer-Verlag, Berlin, vol. 1, part *b*, p. 70, 1977.
55 N. Metropolis, A. W. Rosenbluth, A. H. Teller and E. Teller, *J. Chem. Phys.*, 1953, **21**, 1087.
56 M. P. Allen and D. J. Tildesley, *Computer Simulation of Liquids*, Oxford University Press, New York, 1987.

Paper 4/00564C; *Received* 31*st January*, 1994